SUPPLEMENTARY DATA

Figure S1

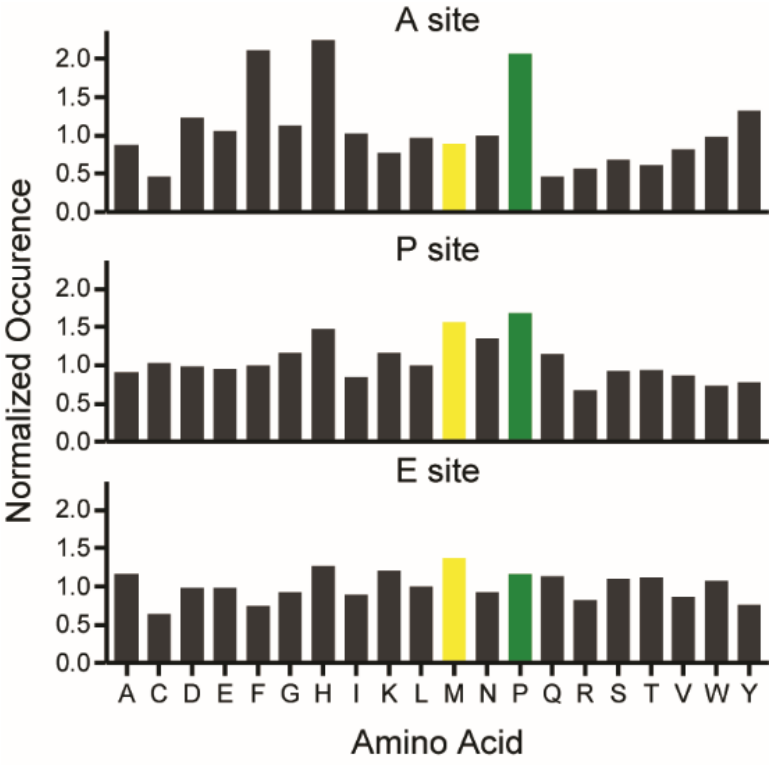

Figure S1 | Occurrence of mRNA codons for each amino acid in the A-, P- and E-site.

(A-C) Ribosomal profiling was performed on the ribosomes from the *in vivo* pullout using the affinity-tagged Ski complex and the normalized occurrence of the mRNA codons for each amino acid in the (A) A-site, (B) P-site, and (C) E-site was calculated.

Figure S2

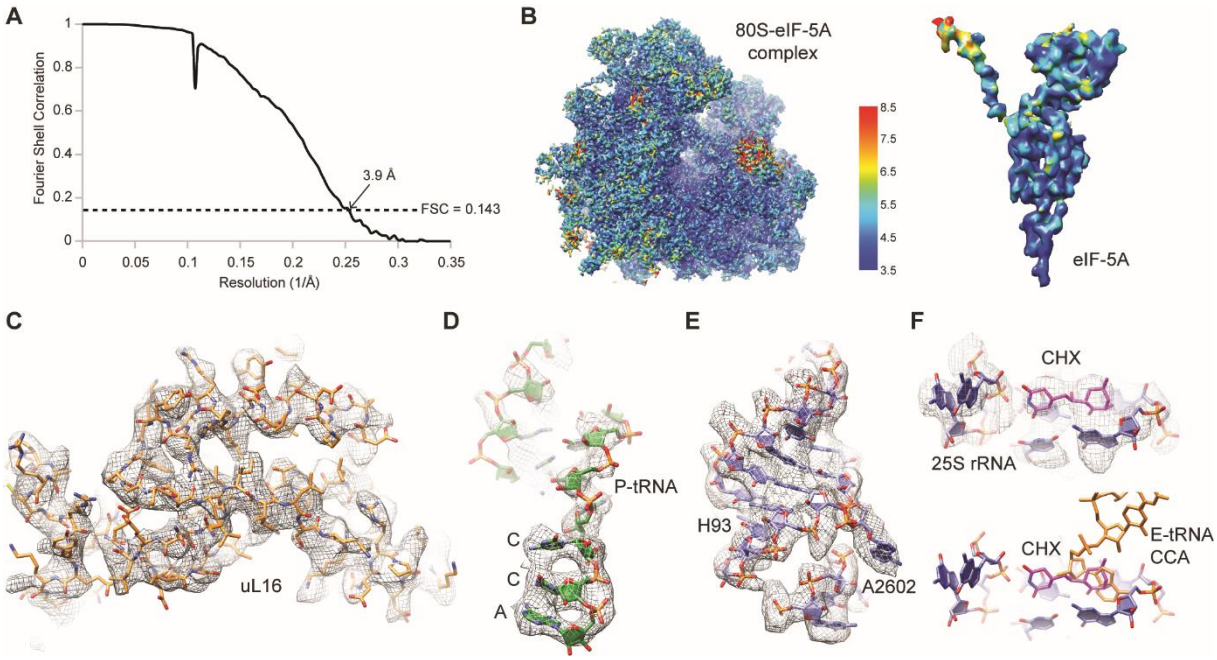

Figure S2 | Resolution of the eIF-5A-80S complex cryo-EM reconstruction. **(A)** Resolution curve for the final cryo-EM map of the eIF-5A-80S complex as obtained from RELION (28). The resolution was determined to 3.9 Å at a FSC cut-off at 0.143 according to the gold-standard criterion. **(B)** eIF-5A-80S map and the isolated density for eIF-5A colored according to the local resolution as obtained by ResMap (30). **(C-E)** Examples densities (grey mesh) and models for (C) uL16 (orange), (D) CCA-end of the P-tRNA (green) and (E) H93 of the 23S rRNA (blue). **(F)** Density for cycloheximide (CHX) in the E-site and the potential clash with the CCA end of an E-site tRNA.

Figure S3

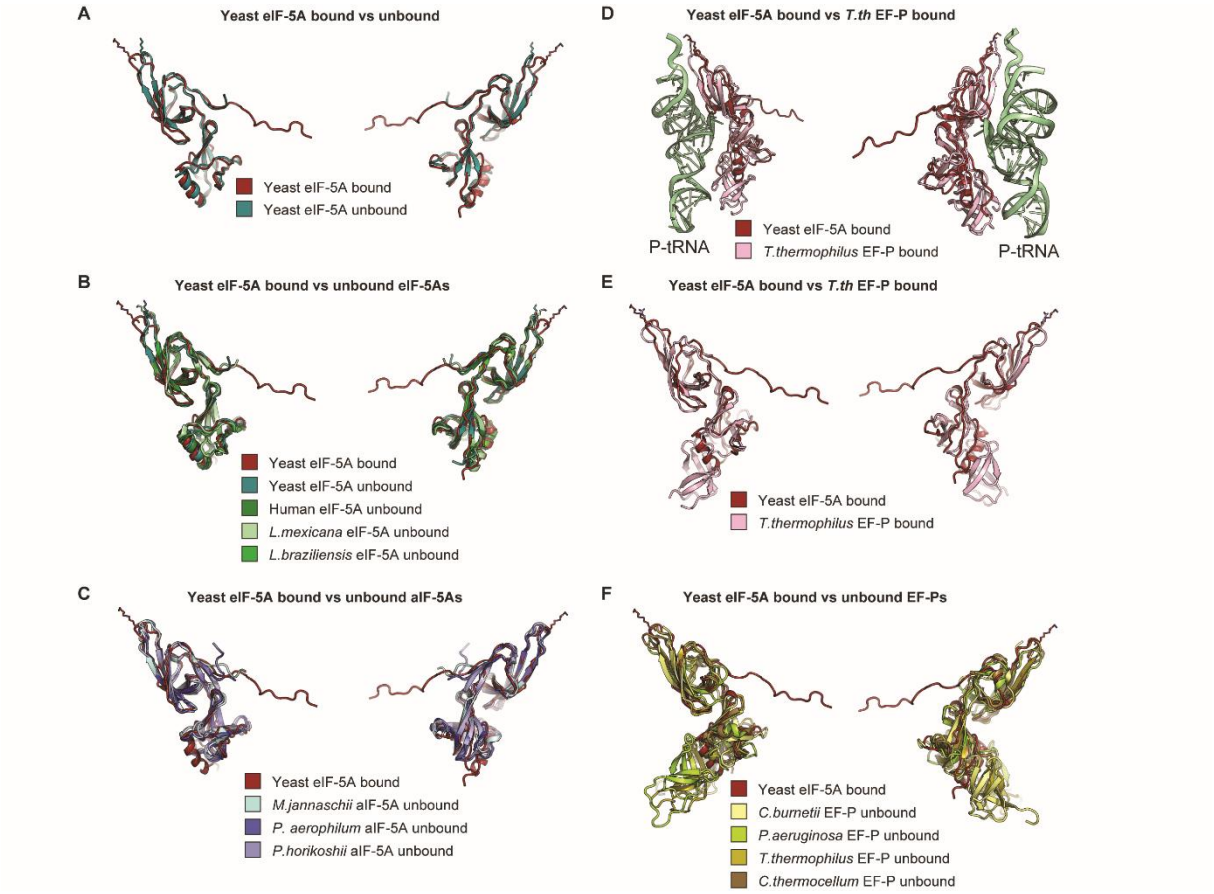

Figure S3 | Comparison of eIF-5A, aIF-5A and EF-P structures.

(A-F) Comparison of the conformation of yeast eIF-5A in complex with the 80S ribosome (bound, red) with (A) crystal structure of free yeast eIF-5A (unbound, green, PDB ID 1ER0), (B) with crystal structures of free eukaryotic eIF-5As from yeast (green, 1ER0), human (49) (green, 3CPF), *Leishmania mexicana* (light green, 1X60) and *L. braziliana* (bright green, 1XTD), (C) with crystal structures of free archaeal aIF-5As from *Methanococcus jannaschii* (59) (cyan, 1EIF), *Pyrococcus horikoshii* (60) (blue, 1I26), and *Pyrobaculum aerophilum* (61) (grape, 1BKB), (D,E) crystal structure of bound *Thermus thermophilus* EF-P (16) (pink, 4U6A) relative P-tRNA (green), and (F) with crystal structures of free forms of bacterial EF-Ps from *Coxiella burnetii* (62) (yellow, 3TRE), *Pseudomonas aeruginosa* (63) (bright green, 3OYY), *Thermus thermophiles* (64) (khaki, 1UEB) and *Clostridium thermocellum* (brown, 1YBY).

Figure S4

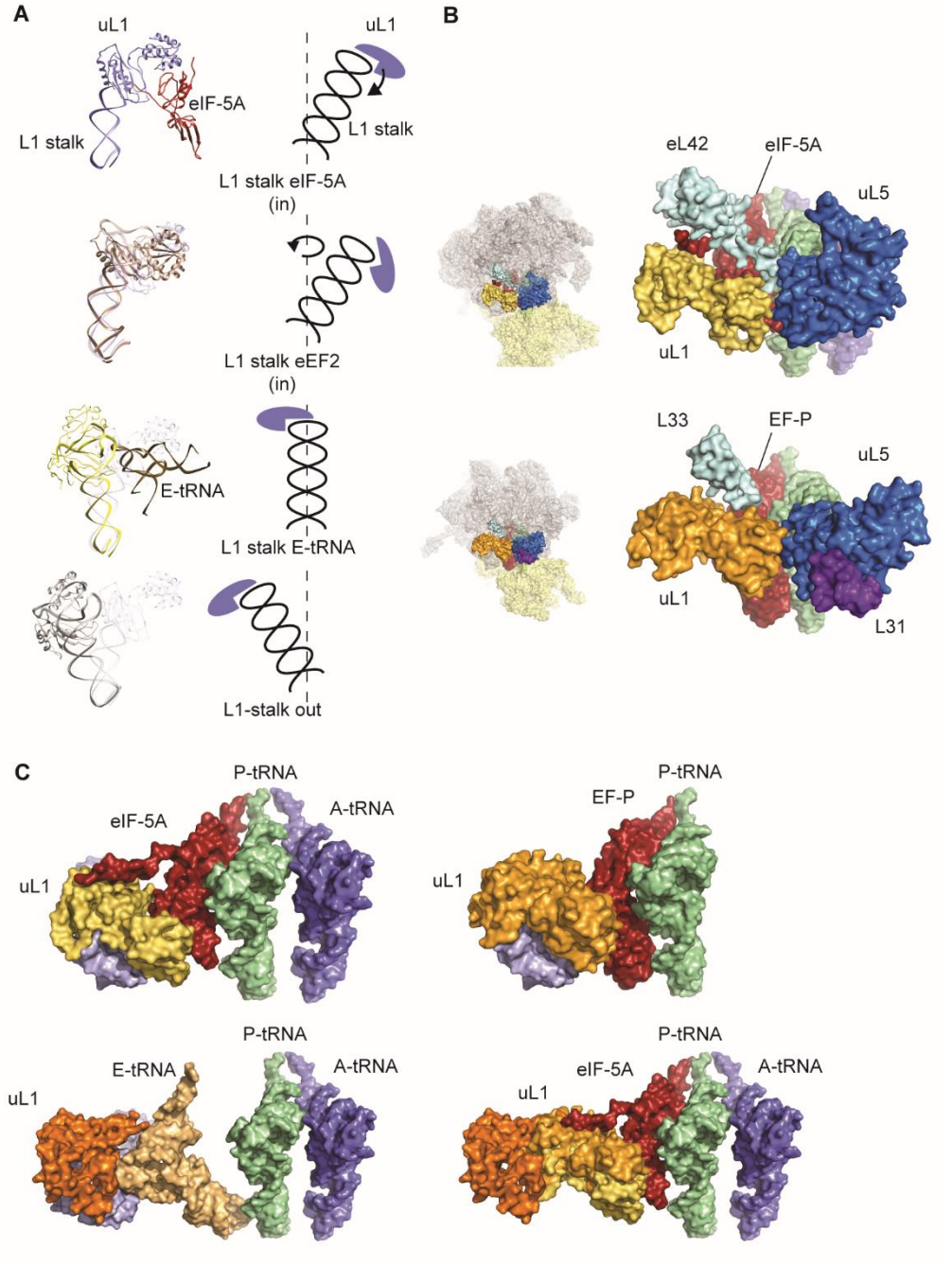

Figure S4 | Comparison of L1 conformations.

(A) Comparison of the L1 stalk conformation in the presence of yeast eIF-5A (upper panel), eEF2 (50) (second row), E-tRNA (48) (third row) and with the uL1 out position observed in stalled wheat germ 80S ribosome (65,66) (lower panel). **(B)** Comparison of uL1 (yellow) in presence eIF-5A (upper panel) compared with uL1 (orange) in presence of EF-P (16) (lower panel). **(C)** Comparison of uL1 (yellow) stalk in presence eIF-5A (top left) compared with uL1 (orange) in presence of EF-P (16) (top

right), or with uL1 (bright orange) in presence of E-tRNA (48) (bottom left). An overlay of uL1 positions is shown in the bottom right panel.

Figure S5

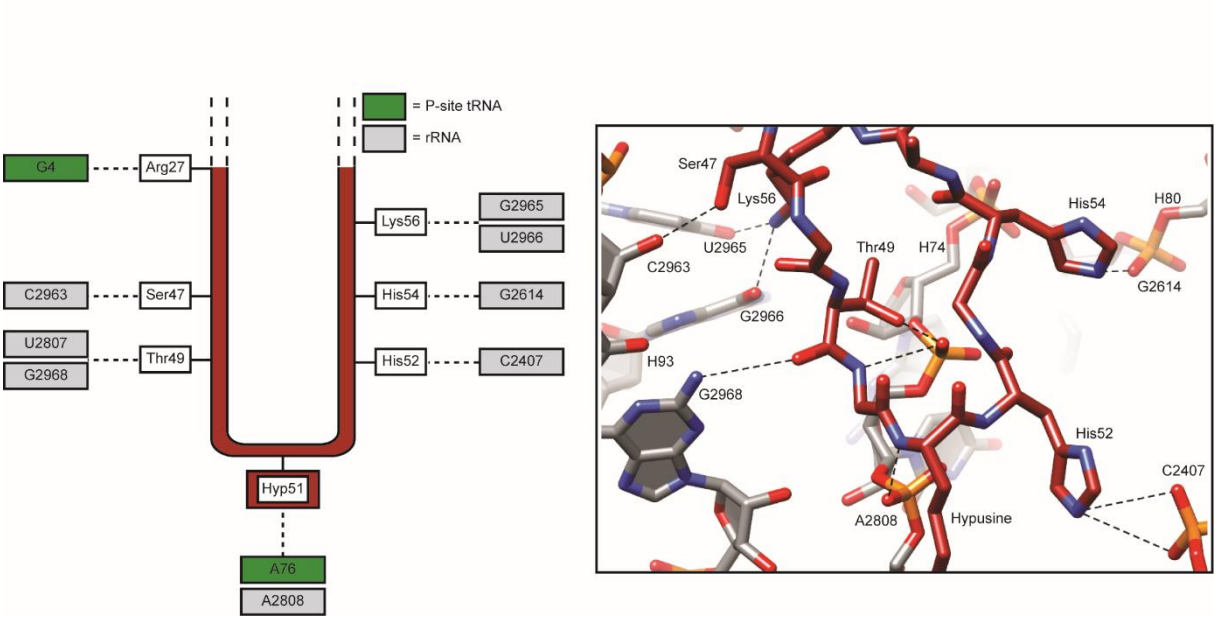

Figure S5 | Interactions between eIF-5A and the 25S rRNA.

(A) Schematic and **(B)** molecular representation of the interactions between eIF-5A (red), P-tRNA (green) and 25S rRNA nucleotides (slate). The interactions with P-tRNA are omitted for clarity in (B).

Figure S6

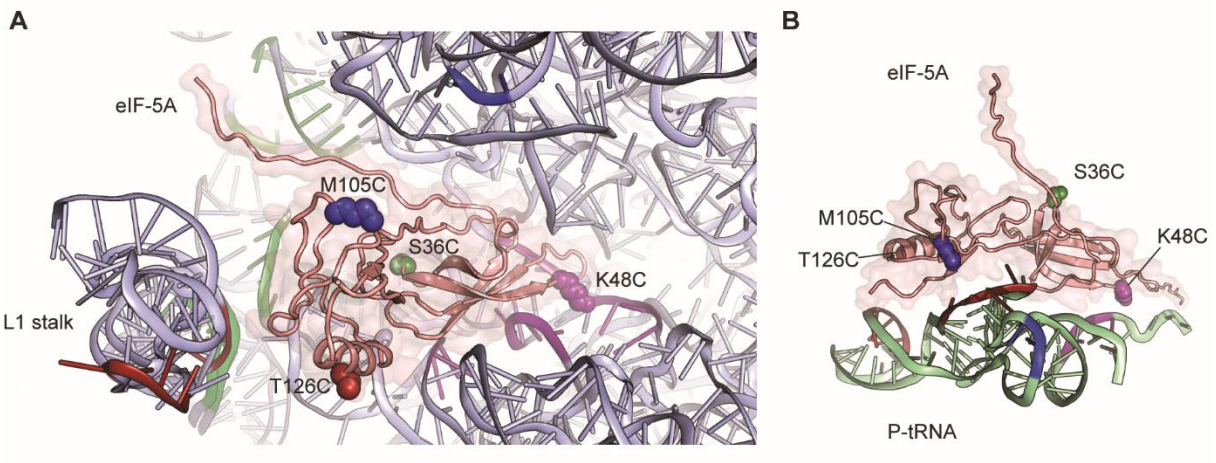

Figure S6 | Hydroxyl-radical probing of eIF-5A.

(A-B) Hydroxyl-radical probing cleavages (7) are mapped onto the (A) 25S rRNA (light blue ribbons) and (B) P-tRNA (green ribbon) from iron tethers located at positions S36 (green), K48 (magenta), M105 (blue) and T126 (red) of eIF-5A (pink ribbons).

Supplementary References

59. Kim,K.K., Hung,L.W., Yokota,H., Kim,R. and Kim,S.H. (1998) Crystal structures of eukaryotic translation initiation factor 5A from Methanococcus jannaschii at 1.8 A resolution. *Proc. Natl. Acad. Sci. U. S. A.*, **95**, 10419–24.
60. Yao,M., Ohsawa,A., Kikukawa,S., Tanaka,I. and Kimura,M. (2003) Crystal structure of hyperthermophilic archaeal initiation factor 5A: a homologue of eukaryotic initiation factor 5A (eIF-5A). *J. Biochem.*, **133**, 75–81.
61. Peat,T.S., Newman,J., Waldo,G.S., Berendzen,J. and Terwilliger,T.C. (1998) Structure of translation initiation factor 5A from Pyrobaculum aerophilum at 1.75 A resolution. *Structure*, **6**, 1207–14.
62. Franklin,M.C., Cheung,J., Rudolph,M.J., Burshteyn,F., Cassidy,M., Gary,E., Hillerich,B., Yao,Z.-K., Carlier,P.R., Totrov,M., *et al.* (2015) Structural genomics for drug design against the pathogen *Coxiella burnetii*. *Proteins Struct. Funct. Bioinforma.*, **83**, 2124-36.
63. Choi,S. and Choe,J. (2011) Crystal structure of elongation factor P from Pseudomonas aeruginosa at 1.75 å resolution. *Proteins Struct. Funct. Bioinforma.*, **79**, 1688–1693.
64. Hanawa-suetsugu,K., Sekine,S., Sakai,H., Hori-takemoto,C., Terada,T. and Unzai,S. (2004) Crystal structure of elongation factor P from Thermus thermophilus HB8. *Proc. Natl. Acad. Sci. U. S. A.*, **101**, 9595–9600.
65. Armache,J.-P., Jarasch,A., Anger,A.M., Villa,E., Becker,T., Bhushan,S., Jossinet,F., Habeck,M., Dindar,G., Franckenberg,S., *et al.* (2010) Cryo-EM structure and rRNA model of a translating eukaryotic 80S ribosome at 5.5-A resolution. *Proc. Natl. Acad. Sci. U. S. A.*, **107**, 19748–19753.
66. Armache,J.P., Jarasch,A., Anger,A.M., Villa,E., Becker,T., Bhushan,S., Jossinet,F., Habeck,M., Dindar,G., Franckenberg,S., et al. (2010) Localization of eukaryote-specific ribosomal proteins in a 5.5-A cryo-EM map of the 80S eukaryotic ribosome. *Proc. Natl. Acad. Sci. U. S. A.*, **107**, 19754–19759.